Effect of heat accumulation on the dynamic range of a gold nanorod doped polymer nanocomposite for optical laser writing and patterning

Peter Zijlstra, James W.M. Chon, and Min Gu

Centre for Micro-Photonics, Faculty of Engineering and Industrial Sciences,
Swinburne University of Technology, P. O. Box 218, Hawthorn, 3122, VIC Australia

JChon@swin.edu.au

Abstract: Even though gold nanorod doped dielectrics have been widely used for optical laser writing and patterning there has been no attempt to study the dynamic range of these nanocomposites, let alone exploring ways to improve this property. Here we study the dynamic range of a gold nanorod doped polyvinyl alcohol film for various laser spot sizes at two different laser pulse repetition rates and show that when a high repetition rate laser source is employed the dynamic range of the nanocomposite is severely limited due to accumulative heating inside the focal volume. This problem could be solved by silica-coating the nanorods inside the polymer matrix. This method does not compromise the high repetition rate of the laser writing source and yet retains the attractive flexible properties of the polymer matrix. The silica-coated gold nanorod doped polymer nanocomposite could be an attractive medium for future high-speed, high repetition rate pulsed laser writing and patterning applications.

© 2007 Optical Society of America

OCIS codes: (160.1190) Anisotropic optical materials; (240.6680) Surface plasmons; (350.5340) Photothermal effects; (210.4770) Optical recording.

References and links

1. M. A. El-Sayed, "Some interesting properties of metals confined in time and nanometer space of different shapes," Acc. Chem. Res. **34**, 257-264 (2001).
2. O. Wilson, G. J. Wilson, and P. Mulvaney, "Laser writing in polarized silver nanorod films," Adv. Mater. **14**, 1000-1004 (2002).
3. J. Pérez-Juste, B. Rodríguez-González, P. Mulvaney, and L. M. Liz-Marzán, "Optical control and patterning of gold-nanorod-poly(vinyl alcohol) nanocomposite films," Adv. Funct. Mater. **15**, 1065-1071 (2005).
4. J. W. M. Chon, C. Bullen, P. Zijlstra, and M. Gu, "Spectral encoding on gold nanorods doped in a silica sol-gel matrix and its application to high density optical data storage," Adv. Funct. Mater. **17**, 875-880 (2007).
5. J. Pérez-Juste, P. Mulvaney, and L. M. Liz-Marzán, "Patterning and encryption using gold nanoparticles," Int. J. Nanotechnol. **4**, 15-225 (2007).
6. S. Link, C. Burda, M. B. Mohamed, B. Nikoobakht, and M. A. El-Sayed, "Laser photothermal melting and fragmentation of gold nanorods: Energy and laser pulse-width dependence," J. Phys. Chem. A **103**, 1165-1170 (1999).
7. S. S. Chang, C. W. Shih, C. D. Chen, W. C. Lai, and C. R. C. Wang, "The shape transition of gold nanorods," Langmuir **15**, 701-709 (1999).
8. B. Nikoobakht, and M. A. El-Sayed, "Preparation and growth mechanism of gold nanorods (NRs) using seed-mediated growth method," Chem. Mater. **15**, 1957-1962 (2003).
9. S. Link, and M. A. El-Sayed, "Spectroscopic determination of the melting energy of a gold nanorod," J. Chem. Phys. **114**, 2362-2368 (2001).

10. H. Petrova, J. Pérez-Juste, I. Pastoriza-Santos, G. V. Hartland, L. M. Liz-Marzán, and P. Mulvaney, "On the temperature stability of gold nanorods: comparison between thermal and ultrafast laser-induced heating," Phys. Chem. Chem. Phys. **8**, 814-821 (2006).
11. F. Cooper, "Heat transfer from a sphere to an infinite medium," Int. J. Heat Mass Transfer, 991-993 (1977).
12. H. Inouye, K. Tanaka, I. Tanahashi, and K. Hirao, "Ultrafast dynamics of nonequilibrium electrons in a gold nanoparticle system," Phys. Rev. B **57**, 11334-11340 (1998).
13. T. Nishino, S. C. Kani, K. Gotoh, and K. Nakamae, "Melt processing of poly(vinyl alcohol) through blending with sugar pendant polymer," Polymer **43**, 2869-2873 (2002).
14. A. Bejan, *Heat transfer* (John Wiley and Sons, 1993).
15. W.J. Roff, and J.R. Scott, *Fibres, films, plastics and rubbers, a handbook of common polymers* (Butterworths, London, 1971).
16. R. C. Weast, and D. R. Lide, *CRC handbook of chemistry and physics*, 85th ed. (CRC press: Boca Raton, Florida, 2004), pp. 4-82.
17. L. M. Liz-Marzán, M. Giersig, and P. Mulvaney, "Synthesis of nanosized gold-silica core-shell particles," Langmuir **12**, 4329-4335 (1996).
18. A. L. Stepanov, D. E. Hole, A. A. Bukharaev, P. D. Townsend, and N. I. Nurgazizov, "Reduction of the size of the implanted silver nanoparticles in float glass during excimer laser annealing," Appl. Surf. Sci. **136**, 298-305 (1998).
19. The parameters used in the equation are ρ_{sil}=2200 kgm^{-3}, k_{sil}=1.3 Wm^{-1}K^{-1}, $c_{p,sil}$=750 Jkg^{-1}K^{-1}.
20. S. Link, C. Burda, M. B. Mohamed, B. Nikoobakht, and M. A. El-Sayed, "Femtosecond transient-absorption dynamics of colloidal gold nanorods: Shape independence of the electron-phonon relaxation time," Phys. Rev. B **61**, 6086-6090 (2000).
21. M. Hu, X. Wang, G. V. Hartland, V. Salgueiriño-Maceira, and L. M. Liz-Marzán, "Heat dissipation in gold-silica core-shell nanoparticles," Chem. Phys. Lett. **372**, 767-772 (2003).

1. Introduction

Metallic nanorods have received much attention because of their anisotropic surface plasmon resonance featuring a large, polarization dependent absorption cross section which can be tuned throughout the visible wavelength range [1]. One of the most promising applications that benefits from these optical properties of gold nanorods is optical laser writing and patterning [2, 3, 4, 5]. Herein the nanorods are embedded in a dielectric matrix and the anisotropy of the embedded particles is exploited by inducing a morphological change from a rod shape into the energetically favored spherical geometry by pulsed laser excitation [6, 7].

In such applications the laser pulse energy is the primary source of shape control, but other factors such as the thermal and mechanical properties of the dielectric matrix also play an important role. In previous studies soft polymer materials such as polyvinyl alcohol (PVA) [2, 3] and ureasils [5] as well as more rigid materials such as silica sol-gel glasses [4] were employed as the matrix material. These nanocomposites have all demonstrated to successfully withstand the particular pulsed laser irradiation conditions.

However, to accommodate the various laser irradiation conditions such as repetition rates and pulse energy densities, it is desirable to study the matrix performance at high power, high repetition rates to ultimately determine the damage threshold conditions. The so-called laser writing dynamic range of the nanocomposite can then be determined by the range bound by recording threshold and damage threshold for a specific irradiation condition.

Even though gold nanorod doped dielectrics have been under intense investigation [2, 3, 4, 5] there has been no attempt to study the dynamic range of these nanocomposites, let alone exploring ways to improve this property imperative to patterning applications. While a polymer such as polyvinyl alcohol (PVA) is an attractive matrix because of its mechanical properties and ease in doping, its low T_g and softness compared to other dielectric materials warrants a low damage threshold and dynamic range. Furthermore, its low thermal conductivity means that it is prone to heat accumulation upon irradiation with a high repetition rate laser source, which significantly limits the dynamic range. These issues need to be resolved for the reliable use of the nanocomposite in optical laser writing and patterning applications.

Here we study both experimentally and theoretically the laser writing dynamic range of a gold nanorod doped PVA film for various laser spot sizes at two different laser pulse repetition rates. We show indeed that at a high repetition rate the heat accumulation in the PVA matrix results in a severely limited dynamic range. We also show that this limited dynamic range can be improved up to 70% by silica coating of the gold nanorods, without compromising the high pulse repetition rate of the laser source. This could be particularly valuable for future high speed laser writing and patterning applications.

This paper is organized as follows. In section 2 we describe the apparatus used in the experiments, and in section 3 the dynamic range of a PVA matrix doped with uncoated gold nanorods at various laser spot sizes is presented. We modeled our system using a two-dimensional heat dissipation model doped with point sources of heat, which is described in section 4, followed by section 5 in which the improvement in the dynamic range of the nanocomposite by silica coating of the nanorods is presented. Finally, concluding remarks are presented in section 6.

2. Experimental

Gold nanorods with an aspect ratio of ∼4.4 were prepared using a silver nitrate assisted, seed mediated growth method, based on the system developed by Nikoobakht et al. [8]. The nanorods were then homogeneously dispersed in a PVA film by mixing a purified nanorod solution (particle concentration ∼2 nM) with a 10% PVA solution, after which 10 μL of the mixture was dropcast on a cover slip and dried at 70 °C. This resulted in a PVA film of about 50 μm thickness with a homogeneous nanorod concentration of ∼25 nM (∼1.5x10^{13} nanorods per cm^3).

Laser writing of patterns was achieved by femtosecond pulsed laser illumination at 850 nm (Spectra-Physics Tsunami, 100 fs pulse widths, 82 MHz repetition rate). The pulse train was focused through a 0.7 NA objective lens. All patterning was conducted 12 μm below the surface. The exposure time was controlled by an electronic shutter and was 25 ms per exposure in all experiments (equivalent to 2.05×10^6 laser shots per exposure). All pulse energies and laser fluences mentioned in the remainder are the values in the focal plane of the objective. Laser fluences indicated are spatially and temporally averaged over a single laser pulse. The patterns were imaged using low power continuous wave illumination at the recording wavelength with a laser scanning microscope operated in transmission (Olympus BX300, 1.2 NA water immersed objective lens). The recording threshold was determined by the lowest laser pulse fluence for which contrast was observed. The damage threshold was identified using a microscope equipped with a white light source and a 100x magnification objective, in which damage was identified as deformation at the surface of the sample.

Absorption spectra of a written bit pattern were measured using a homebuilt micro spectrophotometer. Light from a collimated white light source (Oriel Apex Quartz Tungsten Halogen source) was focused onto the sample through a 1.2 NA water immersed objective and collected in transmission using a 0.8 NA infrared enhanced objective lens. The light was redirected to a spectrograph (Acton Spectrapro 300i) and dispersed onto a charge coupled device (Princeton Instruments PIXIS 100).

3. Effect of NA and laser pulse repetition rate on recording and damage thresholds

In Fig. 1 we show the extinction spectrum of a PVA film doped with gold nanorods with a TEM micrograph of the gold nanorods on a copper grid. The average dimensions of the embedded nanorods are 52 nm x 12 nm leading to an average aspect ratio of 4.4 ± 0.5 (distribution obtained by analyzing >200 particles in TEM micrographs). The inset shows the change in extinction spectrum upon pulsed laser irradiation. Recording was done through a 0.7 NA objective lens using a laser fluence of 7.6 mJcm^{-2}. A clear decrease in extinction is observed around the laser wavelength, whereas the extinction at shorter wavelengths increases. This is consistent

with a recording mechanism based on a shape transformation of the nanorods to lower aspect ratio particles, which is caused by heating and melting of the nanorods [4, 6, 7].

When the pulse energy was further increased we observed significant damage to the nanocomposite upon irradiation. This is displayed in Fig. 2 where we show patterns recorded through a 0.7 NA objective lens using (a) 7.6 mJcm^{-2} and (b) 9 mJcm^{-2}. Using a 0.7 NA objective lens we observe significant deformation in and around the focal volume when the laser fluence exceeded 8.6 mJcm^{-2}.

To investigate the origin of the observed damage we varied the laser spot size by systematically reducing the back aperture of the 0.7 NA objective lens, and identified the recording and damage threshold fluences for each NA value. The results are shown in Fig. 2(c). One would expect that the recording and damage thresholds occur at similar energy densities for all recording NA lenses. Surprisingly, the results in Fig. 2(c) suggest that a higher recording NA requires a higher energy density for recording and damage to occur, i.e., smaller laser spot sizes (high NA focusing) require higher laser fluence to record and damage. Moreover from simple thermodynamic considerations [4] we found that the pulse energy densities employed for recording are not sufficient to cause melting of the embedded gold nanorods. Link et al. [9] reported that it requires ∼65 fJ of absorbed photon energy to heat up a similar sized nanorod to its melting temperature of 1300 K, and Petrova et al. [10] reported that at around 1000 K the nanorods show signs of reshaping. However, we found that the maximum energy absorbed per nanorod to reach the recording threshold (NA 0.7, I∼6.5 mJcm^{-2}) is ∼33 fJ, which corresponds to a maximum temperature rise of ∼600 K. This is well below the melting temperature of gold nanrods for all recording NAs.

Both observations could be indicative of accumulation of heat inside the focal volume by absorption of sequential laser pulses from the high repetition rate laser source. The embedded nanorods act as nanoscale absorbers of the laser energy and transfer their energy to the environment via phonon-phonon interactions. The energy transfer from the nanorods to their environment causes an increase in temperature within the focal volume. The energy then dissipates out of the focal volume into the bulk medium. The time interval between sequential laser
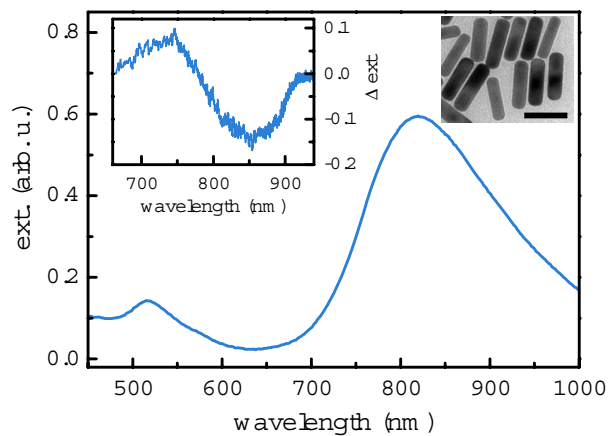

Fig. 1. The extinction spectrum of a PVA film doped with gold nanorods. The TEM micrograph shows the gold nanorods on a copper grid. The scale bar indicates 50 nm. The inset shows the change in optical density within the focal volume upon pulsed laser irradiation (irradiation parameters: NA 0.7, λ = 850 nm, t_{exp}=25 ms, pulse energy density 7.6 mJcm^{-2}.)
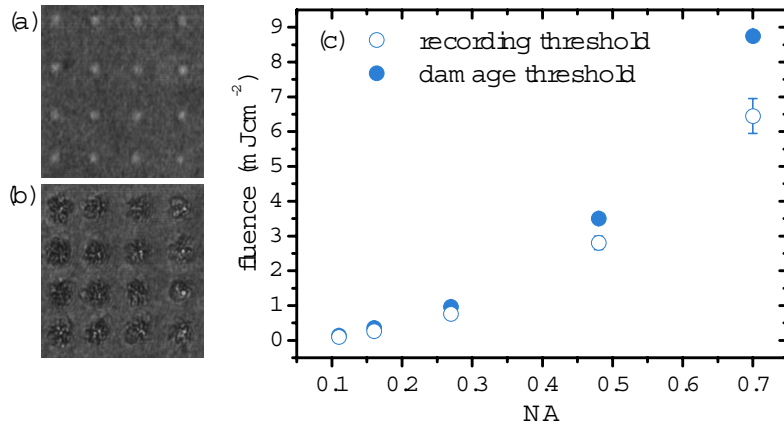
Fig. 2. Bit patterns recorded through an 0.7 NA objective lens using pulse energies of (a) 7.6 mJcm^{-2} and (b) 9 mJcm^{-2}. The size of the whole recorded pattern is 30 μm × 30 μm. (c) Recording threshold (open circles) and damage threshold (solid circles) as a function of NA of the recording lens. The error bars indicate the standard deviation of the spread in contrast obtained from all 16 recorded bits. The error bars for the damage threshold are of the order of the symbol size.

pulses is 12.5 ns, which is significantly shorter than the time required for heat to diffuse out of the focal volume (simulated to be ∼2 μs for a spherical focal volume in PVA with a radius of 1 μm using Cooper's heat dissipation model [11]). Hence over time, the energy from successive laser pulses accumulates in and around the focal volume and causes the PVA to heat up.

As mentioned above, the rise in temperature of the gold nanorods caused by the laser pulses is not enough to reach their melting temperature. However, the temperature of the nanorods embedded in the nanocomposite is governed by both the temperature of the surrounding matrix and the temperature rise induced by the pulsed laser illumination. If the matrix surrounding the nanorods heats up, the additional absorbed laser energy could elevate the temperature inside the nanorods above their melting point. The maximum temperature of the surrounding matrix for recording without damage is limited by the decomposition temperature of PVA, which is ∼540 K [13]. The combined effect of the locally hot matrix and the pulsed laser irradiation (inducing ∆T∼600K, see above) results in a maximum nanorod temperature of ∼1140 K, which is in good agreement with previously reported melting temperatures for similar sized nanorods [9, 10]. The fact that the recording and damage thresholds do not occur at a constant energy density for different NAs (Fig. 2 (c)) indicates that the size of the focal volume plays a critical role in the accumulative heating process. A more quantitative theoretical validation of this observation is discussed in the next section.

To verify experimentally that the effects observed using a high repetition rate laser source are indeed caused by cumulative heating we repeated the above experiment using a low repetition rate laser source (Spectra Physics Spitfire, repetition rate 1 kHz, wavelength 800 nm). Here the inter-pulse separation (1 ms) is significantly longer than the characteristic time for diffusion of heat out of the focal volume (∼2 μs), thus excluding accumulative heating. The recording and damage thresholds obtained using the low repetition rate laser are shown in Fig. 3. The highest NA we used was 0.3 because our power meter did not allow measurement of the extremely low average powers required for the higher NA objective lenses. We observe that the recording and damage threshold occur at similar energy densities for all recording NAs, thus confirming that
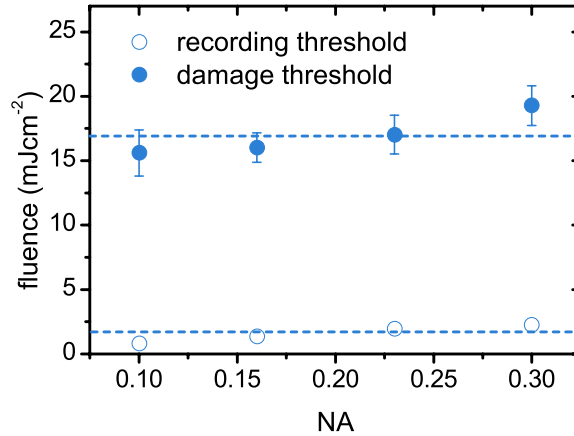
Fig. 3. Recording threshold (open circles) and damage threshold (solid circles) as a function of NA of the recording lens, using a low repetition rate laser source. The error bars for the recording threshold are of the order of the symbol size.

the effects observed using a high repetition rate laser source are due to accumulative heating. The slight increase in threshold observed for increasing NA may be due to the size of the damaged region inside the focal volume being below the detection limit of our imaging system.

4. Theoretical modeling of heat accumulation in the laser focal volume.

To obtain a better insight into the accumulative heating process in a nanoparticle doped dielectric we employed a two dimensional heat dissipation model in which the embedded nanorods were modeled as point absorbers, which is a reasonable assumption on the length scale of several microns. The nanoparticles absorb photon energy, which is converted to thermal energy and dissipated into the surrounding medium. The nanoparticles thus act as point sources of thermal energy. These point sources were homogeneously distributed within an infinite (non-absorbing) PVA matrix with an inter-particle distance of $\sim$400 nm (calculated from the particle concentration in our experiment). The relevant timescales involved [12] are the electron-phonon relaxation time $\tau_{\text{e-ph}}$ (typically < 5 ps) and the phonon-phonon relaxation time $\tau_{\text{ph-ph}}$ (typically > 150 ps). Because $\tau_{\text{e-ph}} << \tau_{\text{ph-ph}}$ it is reasonable to assume that the absorbed energy is released instantaneously by the point source. The generation and dissipation of thermal energy from an instantaneous point source into the PVA gives rise to a time and position dependent temperature change Θ which can be expressed as [14]

$$\Theta(r,t) = T(r,t) - T_0 = \frac{Q}{8\rho c_p (\pi \alpha t)^{3/2}} \exp\left[\frac{-(r-r_0)^2}{4\alpha t}\right], \qquad (1)$$

where T_0 is the initial temperature (293 K), Q is the amount of thermal energy released by the point source, ρ is the density of PVA (1200 kgm^{-3}), c_p is the specific heat capacity of PVA [15] (1650 Jkg^{-1}K^{-1}), $r - r_0$ is the radial distance away from the point source, and α is equal to $k / \rho c_p$ where k is the thermal conductivity of the nanocomposite. The value for the thermal conductivity depends on the volume fraction of nanorods and silica present in the polymer nanocomposite. As in our experiment the combined volume fraction of gold and silica is less than 0.1% we assumed a value for k equal to that for PVA (0.21 Wm^{-1}K^{-1} [15]).

To model the experimentally observed homogeneous dispersion of the nanorods, the point

sources were distributed on a hexagonal grid. To simulate the random alignment of the nanorods in the polymer matrix we assigned a randomly generated Q to each individual nanoparticle. This distribution of Q values was spatially multiplied by a Gaussian function to account for the intensity distribution inside the focal volume. The nanoparticles in the area bounded by twice the full width at half maximum of the Gaussian intensity distribution were included in the calculations.

The time dependent temperature distribution after absorption of a single laser pulse by an ensemble of nanoparticles can be obtained by superposing the solutions for n individual particles. The absorption of subsequent laser pulses at a fixed interval can be calculated by incorporating a temporal offset in Eq. 1.

A typical temperature map of the focal volume obtained from Eq. 1 is shown in Fig. 4(a). The temperature distribution in and around the focal volume was evaluated 12.5 ns after absorption of 200 consecutive laser pulses at a repetition rate of 82 MHz. The random value for Q was set to a maximum of 50 fJ for a nanorod fully aligned to the laser light polarization. Assuming a typical absorption cross section for nanorods [4] of 5×10^{-12} cm^2 this corresponds to an experimental laser fluence of 10 mJcm^{-2}. This amount of absorbed energy is insufficient to completely melt the gold nanorods [9] and thus closely represents our experimental conditions. The Gaussian intensity distribution is shown at the top, the radius r_{foc} was set to 1 μm in this particular case. One can observe a significantly elevated average temperature within r_{foc} due to accumulative heating.

In our experiments we observed that the laser spot size had a profound effect on the degree of accumulative heating (Fig. 2(c)). To verify this observation we varied the theoretical parameter r_{foc} and simulated the temperature profile within the focal volume while keeping the laser pulse fluence constant. The average temperature, defined as the mean temperature within the focal
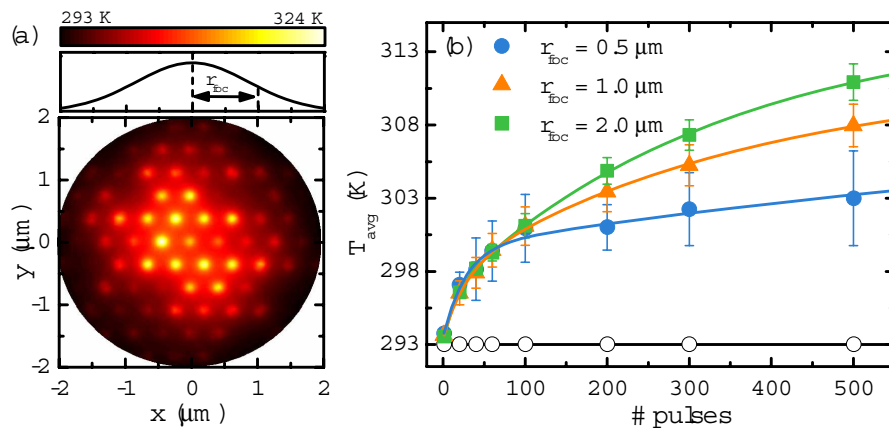

Fig. 4. (a) Typical calculated temperature distribution in and around the focal volume 12.5 ns after absorption of 200 laser pulses at a repetition rate of 82 MHz. The intensity distribution within the focal volume is shown at the top (r_{foc} = 1 μm). (b) Calculated average temperature within the focal volume 12.5 ns after absorption of a number of laser pulses for different r_{foc}. The repetition rate of the laser source was 82 MHz (closed symbols) or 1 kHz (open symbols). The results for different r_{foc} for the low repetition rate laser source overlap. The error bars were obtained by performing fifteen independent calculations for which a new distribution of random Q was defined. The error bars indicate the standard deviation of the spread in T_{avg}.

volume bounded by r_{foc} is then plotted against the number of laser pulses and the results are shown in 4(b). The simulation clearly indicates that the larger the size of the laser focus (i.e., $r_{\text{foc}} = 2 \ \mu$m, NA of focusing objective lens is lower), the more heat accumulates and hence the lower the recording and damage thresholds. This is exactly what was observed in Fig. 2(c). We also simulated the temperature profiles for a low repetition rate (1 kHz) excitation laser source. The simulation did not show any accumulative heating for any r_{foc} or number of laser shots, which confirms our experimental result in the preceding section.

In the initial stages of heat accumulation (< 100 laser pulses or t $< 1 \ \mu$s) we do not observe a significant difference in the rate at which the average temperature increases. This is an effect caused by the spacing between the embedded gold nanoparticles. Thermal energy dissipates away from the gold nanoparticles but due to the low thermal conductivity of PVA the rate at which this thermal energy diffuses is limited. The small heat baths surrounding the nanoparticles have not merged yet and do not interact. Once the small heat baths merge and form a large heat bath the size of the focal volume we observe a significant difference in the rate at which the thermal energy accumulates. A smaller focal spot size has a larger surface to volume ratio and thus has more surface area available for heat to dissipate to the matrix surrounding the focal volume. This results in a lower rate of accumulative heating for smaller focal spot sizes. This confirms our experimental observation that the higher NAs require a higher pulse fluence to obtain resolvable bit contrasts.

5.   Effect of silica coating on the dynamic range

As we have shown in Fig. 2 the observed damage to the nanocomposite material limits the dynamic range of the recording medium (defined as the range of fluences required obtaining 10% to 90% of the maximum achievable contrast) when a high repetition rate laser is employed. It would therefore be favorable to increase the damage threshold and thus the dynamic range of the proposed recording medium. As is shown in Fig. 4(a) the areas with the highest temperature are expected to occur in close proximity to the embedded nanorods. Therefore an effective method to increase the damage threshold and the dynamic range would be to employ a high melting temperature dielectric coating on the nanoparticle surface. Such a method is advantageous for improving thermal properties without compromising the favorable mechanical properties of the polymer matrix. For this purpose we choose silica as the coating dielectric for its high melting temperature [16] ($\sim$1700 K) compared to gold nanorods and PVA. The silica coating is known to withstand the gold nanorod reshaping without deformation, as studied by Chon et al. [4].

Silica coating of the nanorods was achieved using a method previously used to coat gold nanospheres as described by Liz-Marzán et al. [17], which we applied to gold nanorods. The silica shell thickness used in the study described here was 12 nm. Before dispersion into a PVA film the silica coated rods were treated with polyvinylpyrolidine to reduce clustering inside the PVA matrix.

To investigate the effect of a silica coating on the dynamic range of the nanocomposite we recorded patterns using the high repetition rate laser. The laser fluence and the numerical aperture were varied as before and the contrasts obtained are shown in Fig. 5(a). Only contrasts corresponding to patterns without damage to the matrix material are shown. As can be seen a silica coating affects both the recording behavior and the damage threshold of the nanocomposite. The change in recording behavior is caused by the mechanical rigidity of the silica shell, resulting in an increase in pulse energy density required to cause a shape change of the nanorods (i.e. the slope of the curve in Fig. 5(a) is modified). The improved damage threshold of the polymer nanocomposite is attributed to the favorable thermal properties of the silica shell compared to PVA. Also the recording threshold increased slightly due to the stabilizing role of
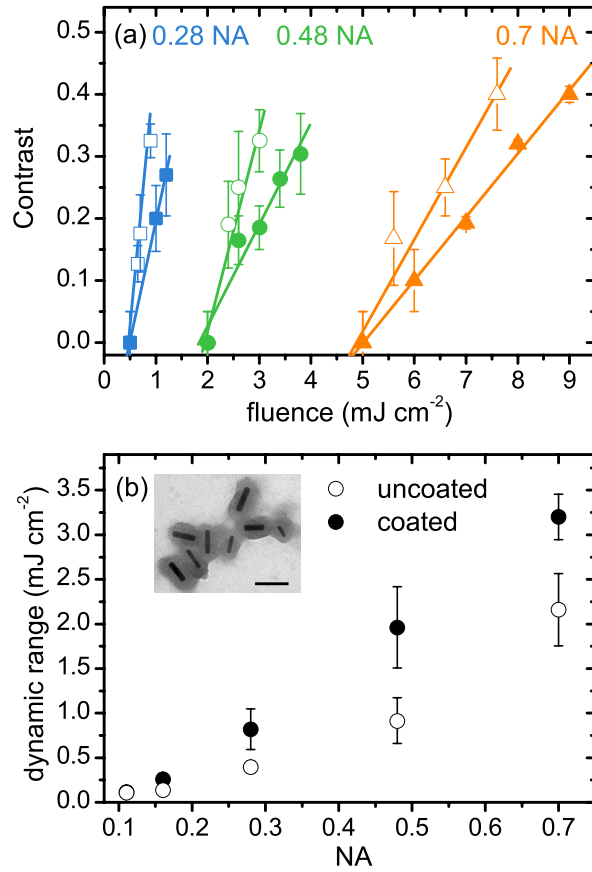
Fig. 5. (a) Bit pattern contrasts obtained from transmission images for patterns recorded with three different numerical apertures in PVA samples doped with uncoated nanorods (open symbols) and silica coated nanorods (solid symbols). The lines are a guide to the eye. The error bars indicate the standard deviation of the spread in contrast obtained from all 16 recorded bits. (b) Dynamic range as a function of NA for PVA samples doped with uncoated gold nanorods (open circles) and silica coated nanorods (solid circles). The inset shows a TEM micrograph of the silica coated nanorods on a copper grid, the scale bar indicates 50 nm.

the rigid silica shell, but this change was small compared to the increase in damage threshold. These effects have resulted in an average increase in dynamic range for a nanocomposite doped with silica coated nanorods of almost 70%, as depicted in 5(b). Also the improvement in dynamic range is larger for higher NAs, which is promising for future development of the laser writing material where higher NA objective lenses are required to pattern finer details at higher resolution.

The large effect of such a thin silica shell can be better understood by considering the temporal evolution of the temperature distribution around the nanoparticles. As a first order approximation we consider the thermal diffusion length R [18], which gives an estimate of the length that heat will diffuse in a time τ,

$$R = \sqrt{\frac{k\tau}{\rho c_p}}, \tag{2}$$

where ρ, c_p, and k are the density, specific heat capacity and thermal conductivity of the silica shell [19]. The diffusion length related to the phonon-phonon relaxation time is important, as this is the timescale on which the majority of the thermal energy is transferred to the surrounding matrix. Based on observation by Link et al. [20] that the gold nanorods and nanoparticles do not differ in electron-phonon and phonon-phonon relaxation times (hence heat transfer) due to the size regime of rods and particles all being equal or less than the mean free path of the electron in gold metal ($\sim$50 nm), the phonon-phonon relaxation time is estimated to be $\sim$80 ps according to the value reported by Hu et al. for gold nanoparticles with a thick, 80 nm silica shell [21]. The thermal diffusion length for a gold nanoparticle in silica is then estimated to be 3.2 nm. This indicates that the highest density of thermal energy is expected in an extremely thin shell surrounding the nanoparticle. Hence the maximum energy density and thus the maximum peak temperature reached in the PVA matrix material is significantly lower when the particles are silica coated, which could explain the significant increase in damage threshold observed in the experiment where the nanorods have a silica shell.

6.   Conclusions

We studied the dynamic range of a gold nanorod doped polyvinyl alcohol film for various laser spot sizes at two different laser pulse repetition rates and showed that when a high repetition rate laser source is employed the dynamic range of the nanocomposite is limited due to accumulative heating inside the focal volume. We also found that the rate at which heat accumulates strongly depends on the size of the focal volume, which was confirmed by theoretical simulations. We proposed a solution to this problem by silica coating of the gold nanorods and showed an increase in dynamic range of 70% when the nanorods were silica coated. The attractiveness of the solution lies in the fact that the nanocomposite can withstand the high repetition rate of the laser source and yet retain the favourable mechanical properties of the polymer matrix. The proposed silica-coated gold nanorod doped polymer nanocomposite is especially attractive for future high-speed, high repetition rate pulsed laser writing and patterning applications.